Vapor–Liquid Equilibrium of the Ternary *n*-Heptane/Isopropyl Alcohol/Atactic Polypropylene Mixture from Perturbation Gas Chromatography

L. L. Joffrion and C. J. Glover*

Department of Chemical Engineering, Texas A&M University, College Station, Texas 77843. *Received July 2, 1985*

ABSTRACT: Multicomponent equation of state polymer solution theories have been in existence for a number of years but have not been widely applied to multicomponent experimental data. This work is a demonstration of the application of two of these theories and the classical Flory–Huggins theory in the polymer-rich concentration regime as well as a demonstration of our recent extension of the chromatographic technique to multicomponent systems. With experiments at 85, 105, and 140 °C, weight fractions of up to 0.05 IPA and 0.11 *n*-heptane were achieved. As would be expected, these random-mixing theories had some difficulty modeling this polar–nonpolar system with the exception of Flory's equation of state, which, by adjusting the segment-surface ratios, fit the data to within experimental error. All theories accurately modeled the binary *n*-heptane/APP system. Results from the ternary mixtures are consistent with poor solvent/solvent miscibility. Optimum interaction parameters are given for the three binary pairs for each theory.

Introduction

Gas chromatography used in conjunction with the classical Flory–Huggins solution theory has been employed to characterize binary polymer solvent mixtures since 1969.[1,2] More recently, equation of state solution theories[3,4,14] have also been applied to binary polymer/solvent experimental data. However, application of these solution theories to ternary (or higher) component mixtures has been limited. The objective of this work was (1) to obtain experimental multicomponent chromatography data in the polymer-rich, finite solvent concentration region for a limited miscibility polymer/two-"solvent" system, and (2) to test the applicability of the previously mentioned solution theories, designed for random mixing, to multicomponent data for this nonrandom mixture.

Gas chromatography was first used to study ternary polymer/solvent mixtures by Bonner and Brockmeier.[5] They obtained experimental data at conditions of infinite dilution in one solvent component, conditions that allow the data to be interpreted with binary chromatography theories. Dincer et al.[6] and Ching[7] both attempted vapor–liquid equilibrium (VLE) determinations of ternary polymer/solvent mixtures but neither accounted for chromatographic interference when both species were at finite concentration. More recently, Ruff et al.[8] presented data for the randomly mixed polybutadiene/benzene/cyclohexane system using the recent extension of the chromatographic technique to multicomponent mixtures by Glover and Lau[9] in which interference is considered. Our new work applies this same theory to a more complex polymer mixture involving both a solvent and nonsolvent.

The basic concepts, theory, and application procedure for perturbation chromatography (also called inverse gas chromatography or elution-on-a-plateau chromatography) with multiple species at finite concentration are given in detail in previous references.[9,10] These results are briefly summarized below for ease of reference and continuity of this paper before presenting the experimental results for the atactic polypropylene (APP) mixtures.

Basic Concepts

In perturbation chromatography, the chromatographic column is perturbed from an initial steady state by injecting a small amount of a component (or components) into the carrier gas stream. This in turn induces a composition perturbation in the stationary phase so as to satisfy equilibrium locally. In multicomponent experiments, these mobile and stationary phase perturbations will separate into several composition perturbations that emerge from the column at different times and are detected in the carrier gas stream as peaks in an appropriate composition-dependent property such as thermal conductivity. The initial operating steady state is achieved by flowing the desired constant composition carrier gas (which may in general contain both nonsorbing and sorbing species) through the column for a sufficiently long period of time for the stationary phase to become saturated with the sorbing species.

The number and composition of the perturbation response peaks depend upon the components in the carrier gas, their equilibria with the stationary phase, and the composition of the perturbation sample injected. The elution time for each peak in general will depend upon both phase equilibrium and mass-transfer rates. Under appropriate experimental conditions of low carrier gas flow rate, however, the effect of the mass-transfer rates on peak retention times can be eliminated,[11] giving the ability to extract equilibrium from measurements of peak retention times.

As an example of one mode of operation for perturbation equilibrium measurements, consider a carrier gas consisting of one inert (nonsorbing) species and two sorbing species. Perturbing the steady-state condition is achieved by injecting a small amount of one or both of the sorbing species. This is the mode that is used for our ternary polymer/two-solvent equilibrium determinations. The upstream perturbation generates two peaks that will proceed through the column at different constant velocities (assuming that operation is achieved that approaches local equilibrium). The extra time (beyond void volume residence time) spent in the column by both of these peaks will depend upon both species' equilibria with the stationary phase and both species' concentrations. We cannot, in this case or in any general multicomponent case, associate any particular peak elution time with any particular species the way we would in infinite dilution chromatography where the sorbing species are absent from the steady-state carrier gas (they are at infinite dilution). This coupling or interference when species are at finite concentration complicates analysis considerably and occurs even if the sorption of each component depends only upon its own concentration.

As a simplification to this example, if one (or both) of the sorbing species is at infinite dilution, then the two

0024-9297/86/2219-1710$01.50/0

peaks decouple in the sense that for each one the elution time depends only upon one of the component's sorption and steady-state concentration. The cases of either infinite dilution or single-component finite concentration perturbation chromatography have been well documented in the literature and comprise the great majority of all previous measurements of equilibrium by chromatography.

Chromatography Theory

Glover and Lau[9] have derived a result applicable to multicomponent sorption that may be used, in conjunction with a solution theory, to characterize the component interactions of the polymeric phase. They assumed local equilibrium, constant temperature, constant pressure, and constant total vapor-phase concentration, one-dimensional flow, small perturbations from steady state, that axial dispersion does not affect retention times, and uniform column packing. For an n-component vapor mixture with all species experiencing sorption they have shown that the $(n-1)$ retention times of the $(n-1)$ response peaks of a particular steady-state composition are related to equilibrium as described by eq 1. Each of the peak residence

$$|(N/M_s)t_r\mathbf{I} + (\mathbf{Y}^* - \mathbf{I})\cdot\beta^* + \mathbf{y}^*\mathbf{b}_n^*| = 0 \qquad (1)$$

times is a root of this equation.

As an example application of this result to multicomponent chromatography data, consider a vapor phase with three components, of which two are sorbing species. Equation 1 in this case is

$$\begin{vmatrix} \frac{N}{M_s}t_r + (y_1^* - 1)\beta_{11}^* + y_1^*\beta_{21}^* & (y_1^* - 1)\beta_{12}^* + y_1^*\beta_{22}^* \\ y_2^*\beta_{11} + (y_2^* - 1)\beta_{21}^* & \frac{N}{M_s}t_r + (y_2^* - 1)\beta_{22}^* + y_2\beta_{12}^* \end{vmatrix} = 0 \qquad (2)$$

The two retention times, which are roots of eq 2, will be known from experimental data. These times arise from the separation of the initial vapor phase perturbation into two equilibrium perturbations that move through the column at their respective velocities to yield two distinct residence times. With these values of residence times known, eq 2 may be viewed as two independent equations (one for each retention time) implicitly expressed in terms of two equilibrium sorption values but explicitly expressed in terms of the four sorption isotherm partial derivatives (β_{11}^*, β_{12}^*, β_{21}^*, β_{22}^*).

Actually determining the isotherms from experimental multicomponent chromatography data is a complex process requiring a set of data at several compositions. At each steady-state composition, there are $(n-1)$ unknowns, the values of stationary phase isotherm equilibrium compositions, for which we have measured $(n-1)$ residence times. However, eq 1 is not explicit in actual sorption compositions but is in terms of $(n-1)^2$ composition derivatives. This means sorption values cannot in general be obtained from experiments at one composition. Rather, data must be obtained at a number of steady-state compositions sufficient to allow fitting the equilibrium sorption isotherm compositions through their derivative values using eq 1.

This method of obtaining the sorption isotherms using eq 1 has been developed by Ruff et al.[10] and applied to a randomly mixed ternary solution.[8] It utilizes solution theories to calculate a set of isotherm partial derivatives and hence peak residence times, by choosing values of the solution theory parameters. A least-squares comparison of these calculated times to the experimental values is used to select optimum parameters. Further details are given in the Appendix.

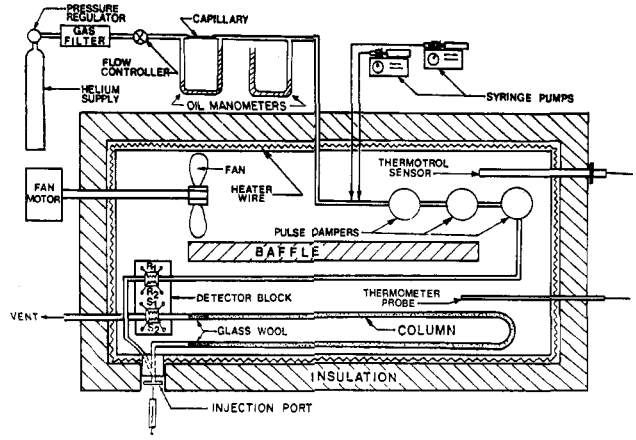

Figure 1. Schematic diagram of the chromatographic apparatus.

Table I
Experimental Data at 84.95 °C

data point	vapor-phase mole fract IPA	vapor flow rate, mol/h	net retention time, min	ave col pressure, bars
1	0.0	0.00977	0.61	1.0071
2	0.1000	0.01029	0.57	1.0121
3	0.2000	0.00778	0.71	1.0033
4	0.3050	0.00651	0.77	1.0106
5	0.4020	0.00907	0.55	1.0109
6	0.4990	0.01027	0.49	1.0095
7	0.5910	0.00867	0.60	1.0095
8	0.7170	0.00715	0.83	1.0078
9	0.8060	0.00953	0.74	1.0099

Materials and Apparatus

Atactic polypropylene was obtained from Hercules Chemical Co. under the brand name AFAX 500. AFAX 500 contains 85–88% atactic polymer chains, 12–15% isotactic chains, and less than 0.1% syndiotactic polymer chains. The sample was purified by dissolving in n-heptane at 98 °C and then separating the resulting solution from the insoluble isotactic residuals. The solvents were reagent-grade chemicals of better than 99% purity.

The experimental data were obtained with the custom-built chromatograph diagramed in Figure 1. The chromatograph column was constructed of 0.318-cm-i.d. 316 stainless steel and was 0.8 m long. The column packing material was Flouropak 80 and was coated with 0.1756 g of polymer using a procedure similiar to that reported by Lau.[12] The polymer coating was 12% by weight. The carrier gas was helium with its flow controlled by an Analab HGC-187 flow controller. The temperature of the oven was controlled to within 50 mK of the desired temperature, and the residence times were measured to the center of mass of the detected peak using a Hewlett Packard 9816 microcomputer.

To assure experimental operating conditions that matched the assumptions of the theoretical development, a low vapor-phase flow rate (0.005–0.015 mol/h), a low column pressure drop ($\Delta p/p \leq 3\%$), and small perturbations of the steady state (injections <0.3 μL) were utilized. For these conditions, retention volumes were independent of flow rate and perturbation size.

Results and Discussion

Experimental data, obtained at 85, 105, and 140 °C, were reduced with the iterative procedure of Ruff et al.[10] The data are given in Tables I–III. The solution theories utilized are (1) the volume and segment fraction approaches to Flory[2] and Huggins[13] theory of polymer solutions, (2) Flory's[14] equation of state, and (3) Sanchez and Lacombe's[3,4] lattice fluid theory. In addition, a modification of Flory's theory given by Bonner and Prausnitz[15] has been used. Equations defining the activity of a multicomponent mixture for each of the above approaches are presented in Table IV. Mixture rules and equations of state are given in Table V. The five models, each

Table II
Experimental Data at 105.65 °C

data point	vapor-phase mol fract		vapor flow rate, mol/h	net retention time,[a] min		ave col pressure, bars
	n-heptane	IPA		peak A	peak B	
1	0.0	0.0	0.00981	2.96 (H)	0.43 (I)	1.0258
2	0.0990	0.0	0.00890	3.22 (H)	0.52	1.0137
3	0.1780	0.0	0.01047	2.77 (H)	0.43	1.0169
4	0.2750	0.0	0.01005	2.89 (H)	0.43	1.0600
5	0.3680	0.0	0.00750	3.85 (H)	0.65	0.9972
6	0.0	0.0900	0.01142	2.62	0.37 (I)	1.0239
7	0.0	0.1800	0.00865	3.23	0.46 (I)	1.0161
8	0.0	0.2590	0.00719	4.00	0.49 (I)	1.0077
9	0.0	0.3590	0.00552	5.24	0.56 (I)	1.0042
10	0.0	0.5070	0.00718	4.16	0.41 (I)	1.0143
11	0.0	0.6000	0.00855	3.39	0.28 (I)	1.0042
12	0.0	0.7020	0.00731	3.94	0.31 (I)	1.0058
13	0.0	0.8010	0.00959	2.99	0.22 (I)	1.0047
14	0.1010	0.0960	0.01079	2.83	0.37	1.0064
15	0.1000	0.1880	0.00828	3.70	0.46	1.0172
16	0.1000	0.3350	0.01087	2.83	0.37	1.0200
17	0.2000	0.1110	0.00932	3.33	0.52	1.0127
18	0.2010	0.2140	0.00927	3.33	0.43	1.0144
19	0.2990	0.1120	0.00922	3.33	0.46	1.0052
20	0.1300	0.6100	0.00841	3.73	0.28	1.0043
21	0.2210	0.6100	0.00841	3.79	0.28	1.0057
22	0.1000	0.7020	0.01094	2.86	0.22	1.0039

[a] H indicates *n*-heptane peak; I indicates isopropyl alcohol peak.

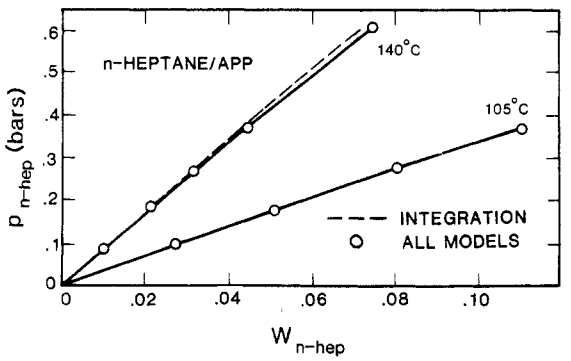

Figure 2. *n*-Heptane partial pressure isotherms of the *n*-heptane/APP mixture at 105 and 140 °C.

involving a solution theory in combination with eq 2, were fit to the experimental data and the results compared. The pure component characteristic constants used for the Flory and Sanchez and Lacombe theories are given in Table VI.

In addition to the use of the solution theories, data for the two binary polymer mixtures of this study have been reduced by numerically interpolating the isotherm derivatives (which may be obtained directly from the binary data) and integrating the derivative interpolating polynomial to obtain the equilibrium isotherm compositions of the binary mixtures. This procedure removes model dependence from the isotherm determination.

Solution Modeling Results. The results obtained from the polymer/solvent binary mixture data are shown graphically in Figures 2–5. In addition, Table VII gives the polymer solvent interaction parameters obtained from optimizing each of the model's fit to the experimental data.

Figure 2 shows the isotherm compositions calculated for the *n*-heptane/APP mixture. For this mixture, the equilibrium isotherm compositions determined with the various models were essentially the same values. Also, the model-independent determination of compositions yielded comparable results. Experimental data at 85 °C for the *n*-heptane/APP solution were not obtained due to the vapor pressure limitations of *n*-heptane.

In Figure 3, results are shown for the isopropyl alcohol (IPA)/APP mixture. At temperatures of 140 and 105 °C

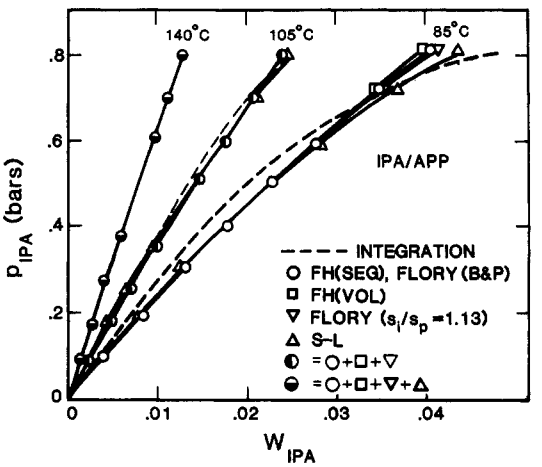

Figure 3. IPA partial pressure isotherms of the IPA/APP mixture at 85, 105, and 140 °C.

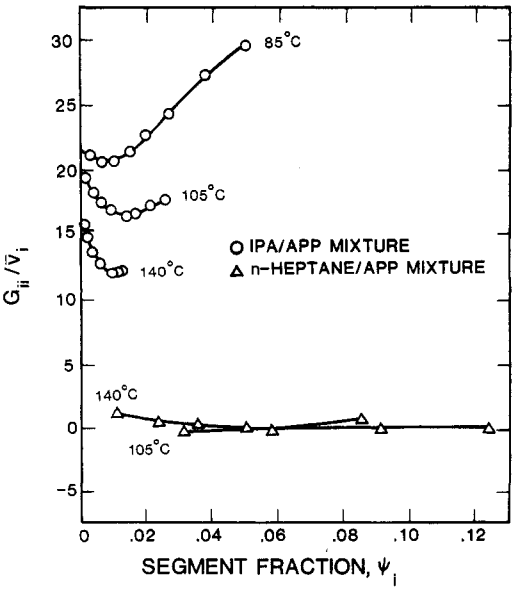

Figure 4. Cluster function values of IPA and *n*-heptane in APP at 85, 105, and 140 °C.

Table III
Experimental Data at 140.15 °C

data point	vapor-phase mol fract		vapor flow rate, mol/h	net retention time,[a] min		ave col pressure, bars
	n-heptane	IPA		peak A	peak B	
1	0.0	0.0	0.00748	1.62 (H)	0.34 (I)	1.0075
2	0.0	0.0930	0.01110	1.11	0.22 (I)	1.0401
3	0.0	0.1750	0.00589	2.10	0.40 (I)	1.0133
4	0.0	0.2690	0.00580	2.09	0.34 (I)	1.0198
5	0.0	0.3670	0.00992	1.23	0.19 (I)	1.0436
6	0.0	0.6140	0.00594	2.01	0.20 (I)	1.0055
7	0.0	0.7020	0.00731	1.75	0.14 (I)	1.0055
8	0.0	0.7980	0.00963	1.20	0.08 (I)	1.0055
9	0.0870	0.0	0.00634	1.78 (H)	0.40	0.9993
10	0.1820	0.0	0.00599	1.75 (H)	0.43	1.0088
11	0.2670	0.0	0.00698	1.42 (H)	0.37	1.0078
12	0.3710	0.0	0.00745	1.20 (H)	0.37	1.0077
13	0.6040	0.0	0.00670	1.05 (H)	0.35	1.0091
14	0.0940	0.0890	0.01158	0.98	0.21	1.0298
15	0.0910	0.1700	0.00916	1.29	0.25	1.0111
16	0.0910	0.2520	0.00611	1.86	0.38	1.0091
17	0.1780	0.0990	0.01044	1.04	0.25	1.0215
18	0.1800	0.1920	0.01031	1.04	0.21	1.0233
19	0.2800	0.1040	0.00987	1.05	0.23	1.0105
20	0.1380	0.6040	0.00848	1.42	0.12	1.0091
21	0.2190	0.6040	0.00849	1.40	0.11	1.0063
22	0.0990	0.7020	0.01095	1.13	0.06	1.0064

[a] H indicates *n*-heptane peak; I indicates isopropyl alcohol peak.

Table IV
Solution Model Equations[a]

model	solution activity (a_i^s)
F–H(VOL)[b]	$\phi_i \exp\sum_j(1-(r_i/r_j))\phi_j - \sum_{j=1}^{n-1}\sum_{k=j+1}^{n}\phi_j\phi_k\chi_{jk}r_i/r_j + \sum_j\phi_j\chi_{ij}$
F–H(SEG)[c]	$\Psi_i \exp\sum_j(1-(r_i/r_j))\Psi_j - \sum_{j=1}^{n-1}\sum_{k=j+1}^{n}\Psi_j\Psi_k\chi_{jk}r_i/r_j + \sum_j\Psi_j\chi_{ij}$
Flory EOS[d]	$\Psi_i \exp\sum_j(1-(r_i/r_j))\Psi_j + (M_iv_{isp}^*/RT)p_i^*[3\tilde{T}_i \ln[(\tilde{v}_i^{1/3}-1)/(\tilde{v}^{1/3}-1)] + \tilde{p}_i - \tilde{p} + \tilde{p}_i(\tilde{v}-\tilde{v}_i] - \tilde{p}\sum_{j=1}^{n-1}\sum_{k=j+1}^{n}\theta_j(s_i/s_j)X_{jk}\theta_k + \tilde{p}\sum_j\theta_jX_{ij}$
simplified Flory[e]	$\Psi_i \exp\sum_j(1-(r_i/r_j))\Psi_j + (M_iv_{isp}^*/RT)p_i^*[3\tilde{T}_i \ln[(\tilde{v}_i^{1/3}-1)/(\tilde{v}^{1/3}-1)] + \tilde{p}_i + \tilde{p}_i(\tilde{v}-\tilde{v}_i)] + \tilde{p}\sum_j\sum_k\Psi_j\Psi_kp_{jk}^* - 2\tilde{p}\sum_j\Psi_jp_{ji}^*$
Sanchez-Lacombe[f]	$\Psi_i \exp\sum_j(1-(r_i/r_j))\Psi_j - (M_iv_{isp}^*/RT)p_i^*[\tilde{p}_i - \tilde{p} + \tilde{p}_i(\tilde{v}-\tilde{v}_i) + \tilde{T}_i[(\tilde{v}-1)\ln(1-\tilde{p}) - (\tilde{v}_i-1)\ln(1-\tilde{p}_i)]] + (\tilde{p}/2)\times\sum_j\sum_k\Psi_j\Psi_k^*\Delta P_{jk} - \tilde{p}\sum_j\Psi_j\Delta p_{ji}^* + \ln\tilde{p}/\rho_i$

[a] Summations are from 1 to n unless otherwise indicated. [b] $\chi_{ij} = \chi_{ji}r_i/r_j$; $r_i/r_j = M_iv_{isp}/M_jv_{jsp}$. [c] $\chi_{ij} = \chi_{ji}r_i/r_j$; $r_i/r_j = M_iv_{isp}^*/M_jv_{jsp}^*$. [d] $\chi_{ij} = (s_i/s_j)X_{ji}$; $r_i/r_j = M_iv_{isp}^*/M_jv_{jsp}^*$; $\theta_j = \Psi_j/\sum_k\Psi_k(s_k/s_j)$. [e] $p_{ij}^* = p_{ji}^*$; $p_{ii}^* = p_i^*$, the pure component value. [f] $\Delta p_{ij}^* = p_i^* + p_j^* - 2p_{ij}^*$; $\Delta p_{ii}^* = 0$; $r_i/r_j = M_iv_{isp}^*/M_jv_{jsp}^*$; Sanchez and Lacombe define a dimensionless parameter $X_{ij} = \Delta p_{ij}^*/(p_i^*\tilde{T}_i)$.

Table V
Mixture Rules and Equations of State for the Solution Models

model	mixture rules	equation of state
F–H(VOL), F–H(SEG)	none	none
Flory	$p^* = \sum_i\Psi_ip_i^* - \sum_{i=1}^{n-1}\sum_{j=i+1}^{n}\Psi_iX_{ij}\theta_j$ $T^* = p^*/[\sum_i\Psi_ip_i^*/T_i^*]$	$\tilde{p}\tilde{v}/\tilde{T} = [\tilde{v}^{1/3}/(\tilde{v}^{1/3}-1)] - 1/(\tilde{v}\tilde{T})$
simplified Flory	$p^* = \sum_i\sum_j\Psi_i\Psi_jp_{ij}^*$ $T^* = p^*/[\sum_i\Psi_ip_i^*/T_i^*]$	(same as Flory)
Sanchez–Lacombe[a]	$p^* = \sum_i\Psi_ip_i^* - \sum_{i=1}^{n-1}\sum_{j=i+1}^{n}\Psi_j\Psi_k\Delta p_{jk}^*$ $T^* = p^*\sum_i\Psi_i^\circ T_i^*/p_i^*$	$\tilde{p}^2 + \tilde{p} + \tilde{T}[\ln(1-\tilde{p}) + (1-(1/r))\tilde{p}] = 0$

[a] $\Psi_i^\circ = (\Psi_ip_i^*/T_i^*)\sum_j(\Psi_j^\circ T_j^*/p_j^*)$ and $1/r = \sum_j(\Psi_jp_j^*/r_j^\circ T_j^*)\sum_k(\Psi_k^\circ T_k^*/p_k^*)$

the isotherms calculated with all the models are approximately the same, though a small difference occurs at 105 °C. However, at 85 °C, a distinct difference exists between the model-independent isotherm and the solution theory isotherms. The model-independent isotherm compositions may be taken as correct within experimental error, thus implying that the solution theories, each derived on the basis of random molecular mixing, do not adequately describe the VLE behavior of the polar IPA/APP mixture. The behavior of this mixture is substantially a result of the hydrogen bonds existing between the IPA molecules which cause these molecules to group together in the solution. This nonrandom mixing yields molecular interactions not completely describable by the random mixing solution theories used to fit the equilibrium isotherms.

The grouping or clustering of the IPA molecules is illustrated in Figure 4, where the cluster function of Zimm[16] is plotted vs. segment fraction of IPA in APP. The form of Zimm's cluster function plotted in Figure 4 is given in eq 3. The high values of the cluster function for IPA in

$$G_{ii}/\bar{V}_i = -\phi_j[\partial(a_i/\phi_i)/\partial a_i] - 1 \quad (3)$$

APP indicate molecular grouping or clustering of IPA molecules. As would be expected, the cluster function values for *n*-heptane in APP are small, indicating very little grouping of *n*-heptane molecules.

Literature experimental data for these polymer/solvent systems are limited. There seem to be no studies of the IPA/APP system published and two studies reported involving the *n*-heptane/APP system.[17,18] Both studies of the *n*-heptane/APP system reported have been conducted at 25 °C using calorimetric measurements; however, these studies were conducted with dissimilar samples of APP. Ochiai et al.[18] report Flory's X_{ip} parameter to be 3.50

Table VI
Solution Theory Constants[a]

	volume, cm^3/g	characteristic pressure, MJ/m^3	temp, K
	Flory		
n-heptane	1.14	385.0	4840
IPA[b]	1.01	559.0	5349
APP	1.00	853.4	6940
	Sanchez and Lacombe		
n-heptane	1.25	309.0	487
IPA	1.02	853.2	399
APP[c]	1.13	257.5	644

[a] Except where indicated the characteristic values were obtained from Bonner and Prausnitz[15] for Flory's EOS and from Sanchez and Lacombe[3] for their EOS. [b] IPA characteristic values for use in Flory's EOS were calculated with the characteristic values and eq 24b, 25b, and 26b of ref 3 to determine $T\alpha$ and $P\beta$. Values of $T\alpha$ and $P\beta$ were then used in equations 25, 26, and 27 of ref 15 to yield the desired characteristic values. [c] APP characteristic values for use in Sanchez and Lacombe's EOS were calculated with the characteristic values and eq 5 and 25 of ref 15 to obtain $T\alpha$. $T\alpha$ was subsequently used with Table II of ref 22 and eq 25b of ref 3 to yield the desired characteristic values.

Table VII
Optimum IPA/APP and *n*-Heptane/APP Interaction Parameters[a]

solution theory	IPA/APP			*n*-heptane/APP	
	85 °C	105 °C	140 °C	105 °C	140 °C
F-H(VOL)	1.953	1.610	1.036	-0.1766	-0.2534
F-H(SEG)	2.093	1.790	1.302	0.0587	0.0460
Flory(B&P)	647.7	653.1	663.7	476.0	477.0
FEOS	118	106	85	-8.2	-10.1
s_i/s_p	1.13	1.13	1.13	1.06	1.06
FEOS	137	119	91	-7.6	-8.8
s_i/s_p	3.65	3.80	4.15	0.70	0.75
S-L	74	58	25	-6.0	-8.5

[a] All units are MJ/m^3 except for F-H(VOL) and F-H(SEG), which are dimensionless.

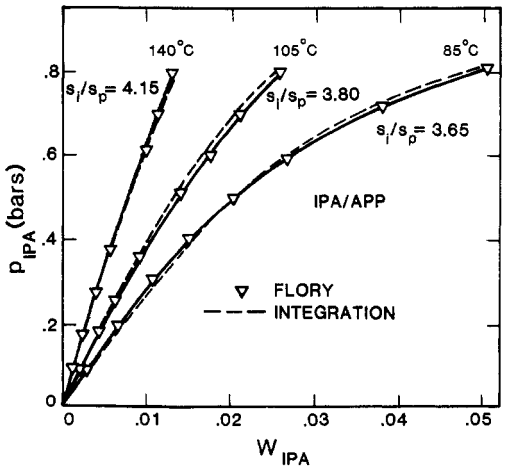

Figure 5. IPA partial pressure isotherms of the IPA/APP mixture at 85, 105, and 140 °C, calculated with optimum segment surface ratios in the Flory model.

MJ/m^3 at 25 °C, and Phuong-Nguyen and Delmas[17] report the same parameter to be 0.29 MJ/m^3. Considering the temperature dependence of X_{ip}, our values are in agreement with those reported at the lower temperature. Additionally, Brockmeier et al.[19] conducted VLE studies using gas chromatography on the hexane/APP system at 80 °C. The isotherm they reported for the hexane/APP system

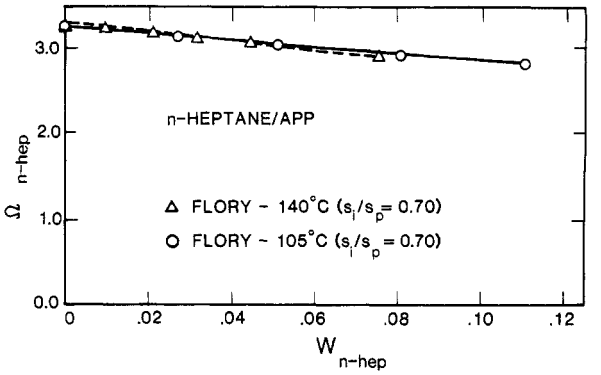

Figure 6. *n*-Heptane weight fraction activity coefficients of the *n*-heptane/APP mixture at 105 and 140 °C.

exhibits similar behavior to those of the present work with *n*-heptane/APP.

Optimum Flory Model. The Flory[14] EOS isotherm shown in Figure 3 for the IPA/APP equilibrium composition was determined with a segment surface ratio, s_i/s_p (i.e., solvent to polymer) of 1.13 as calculated from the results of Bondi.[20] However, in Figure 5, Flory[14] isotherms are shown that were determined by adjusting the s_i/s_p ratio and optimizing the interaction parameter X_{ip} until the best fit using these two parameters was obtained. These Flory[14] isotherms compare very well with the model-independent isotherm. The values of s_i/s_p and X_{ip} used to calculate the isotherms shown in Figure 5 are given in Table VII. Clearly, a superior fit to the polar IPA/APP is obtained by treating the ratio s_i/s_p as an additional parameter of the solution model. No significant difference in the fit of the *n*-heptane/APP data using this two parameter approach was found.

The modeling results obtained by using the Flory[14] EOS as a two-parameter model (i.e., X_{ip} and s_i/s_p) were sensitive to the s_i/s_p value for the IPA/APP mixture data but insensitive to s_i/s_p for the *n*-heptane/APP data. The sensitivity of this random two-parameter model to the s_i/s_p value for IPA/APP, a nonrandom solution, tends to lessen the physical significance of the s_i/s_p ratio, as may be observed by the large values for this case (3.65, 3.85, and 4.14). In addition, for the nonrandom solution of IPA/APP, this sensitivity makes a priori estimation of solution behavior difficult unless an accurate estimation of s_i/s_p is available. However, for the random solution of *n*-heptane/APP, the insensitivity of the results to s_i/s_p values implies that only X_{ip} need be known to reasonably estimate solution behavior.

Mixture Thermodynamic Characteristics. With reference again to the equilibrium compositions shown in Figures 2 and 5, clearly *n*-heptane is more soluble in the polymer than IPA. The highest concentration of IPA in APP is approximately 0.05 wt % at an IPA partial pressure of 0.8 bar and 85 °C. The highest *n*-heptane concentration, however, reaches 0.11 wt % at only 0.38 bar and 105 °C, conditions of lower partial pressure and higher temperature.

The difference in solubility is also reflected in the values of the solvent/polymer interaction parameters shown in Table VII. The parameter values for *n*-heptane/APP are significantly lower than those for IPA/APP. The significance of this trend is most clearly evident from the parameter values for the Flory–Huggins model. These χ values determined for IPA/APP are much greater than 0.5 (the theoretical upper limit for miscibility), indicating poor miscibility. However, the χ values for *n*-heptane/APP are less than 0.5, indicating good miscibility. This difference in solvent solubility in APP is completely con-

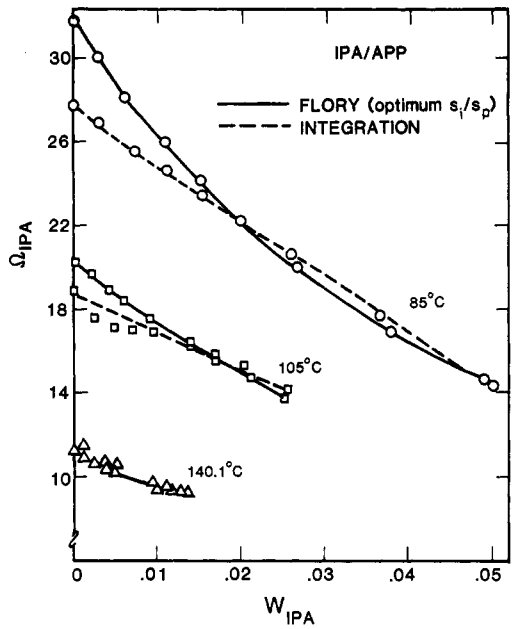

Figure 7. IPA weight fraction activity coefficients of the IPA/APP mixture at 85, 105, and 140 °C.

Table VIII
Optimum IPA/*n*-Heptane Interaction Parameters[a]

solution theory	105 °C	140 °C
F-H(VOL)	4.220	2.585
F-H(SEG)	4.377	3.133
Flory(B&P)	540.5	502.2
FEOS	142	214
s_i/s_j	0.94	0.94
FEOS	6.9	122.3
s_i/s_j	0.18	0.18
S-L	111	171

[a] All units are MJ/m^3 except for F-H(VOL) and F-H(SEG), which are dimensionless.

sistent with the known mixing characteristics of polar and nonpolar mixtures.

Activity coefficients, Ω, of the solvents in their respective binary mixtures are shown in Figures 6 and 7. These activity coefficients were determined with the optimum Flory theory as described above. The wide difference in activity coefficients for the two mixtures is essentially a result of polarity and vapor-pressure differences between the two solvents.

Figures 8–10 show results for the ternary mixtures, which also are consistent with poor miscibility in this system. The solvent/solvent interaction parameters obtained from fitting the solution models to the data are given in Table VIII. The values of these parameters are consistent with poor IPA/*n*-heptane miscibility, an implication most clearly evident from the interaction parameter value of the Flory–Huggins model, as noted above. Figure 8, parts a and b, are plots of individual solvent partial pressures vs. that solvent's weight fraction in the polymer phase at 105 and 140 °C, respectively.

Figure 8c is a comparable plot for the benzene/cyclohexane/polybutadiene data reported by Lau.[21] Note for this mixture that adding benzene to the solution at a fixed partial pressure of cyclohexane increases cyclohexane sorption. This enhanced cyclohexane sorption upon the addition of benzene (and vice versa) is a result of the binary pairs being mutually soluble. Figure 8, parts a and b, showing results of the present work, indicate far less mutual solubility.

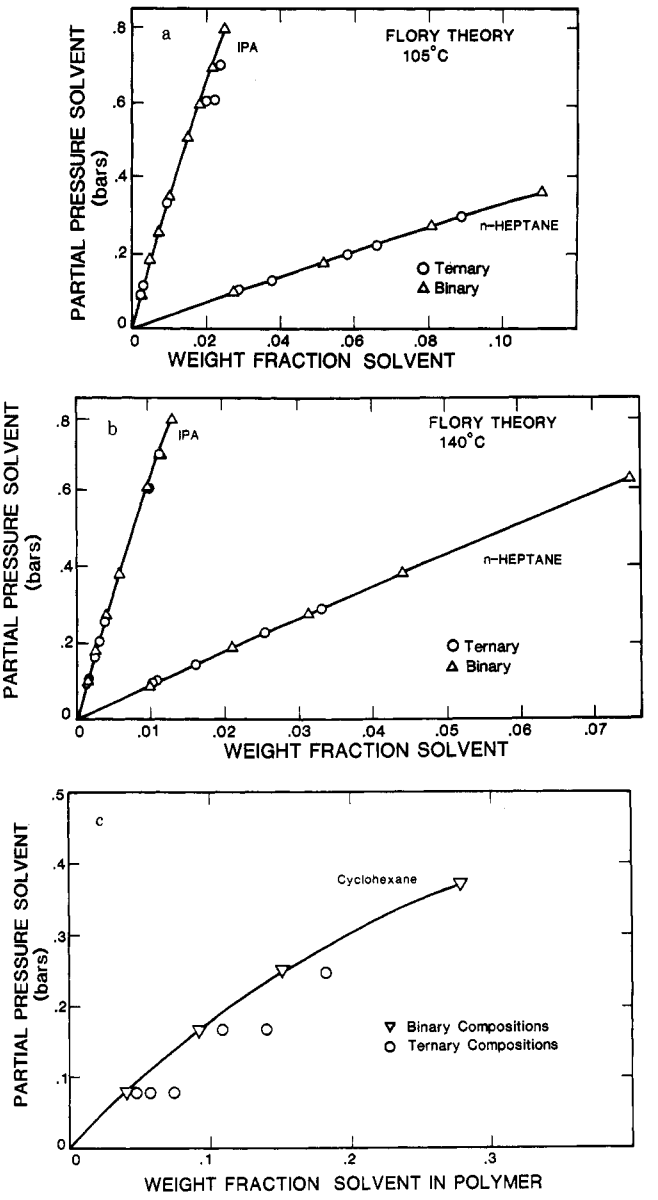

Figure 8. Binary partial pressure isotherms of the indicated solvents showing relative position of similiar composition results but from the ternary mixture: (a) at 105 °C; (b) at 140 °C; (c) cyclohexane/polybutadiane isotherms at 60 °C showing ternary mixture compositions of the cyclohexane/polybutadiene/benzene solution.

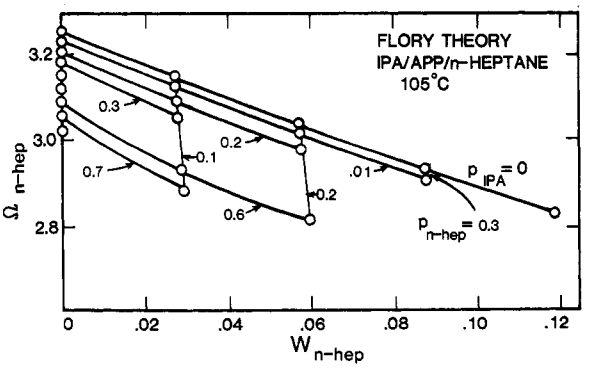

Figure 9. *n*-Heptane weight fraction activity coefficients of the ternary mixture at 105 °C.

Finally, Figures 9 and 10 provide examples of the solvent's activity coefficient behavior in the ternary mixture at 105 °C. The solid lines in each figure are lines of constant partial pressure of the indicated solvent component. Each of these figures shows, for constant partial pressure

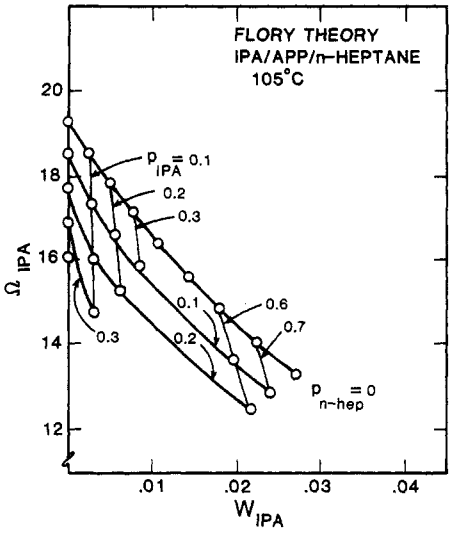

Figure 10. IPA weight fraction activity coefficients of the ternary mixture at 105 °C.

of one solvent component, that addition of the other solvent to the mixture decreases the activity coefficient of the one solvent in that mixture. The solvent activity coefficient behavior at 140 °C (not shown) is similar to that at 105 °C.

Conclusions

For the APP/*n*-heptane/IPA ternary system, repeatable experimental multicomponent chromatography data have been obtained under operating conditions satisfying the assumptions of low pressure drop, constant temperatures, negligible mass transfer resistance, small perturbations from steady state, and uniform column packing. Applicability of several solution theories to the data has been tested. The Flory–Huggins theory, the simplified Flory theory, and Sanchez and Lacombe's lattice fluid theory do not adequately model the VLE behavior of this nonrandom mixture. However, The Flory equation of state theory, when the segment surface ratio is treated as an additional adjustable parameter, adequately describes the VLE behavior of this mixture. In addition, the results of the data and the values of the model parameters are consistent with known mixing characteristics of polar and nonpolar compounds and demonstrate the extension of the chromatographic technique to multicomponent mixtures of limited miscibility.

Acknowledgment. This material is based upon work supported in part by the National Science Foundation under Grant CPE-8111272.

Appendix. Isotherm Determination by Parameter Estimation

Equation 2 relates partial derivatives of the sorption surfaces to chromatographic retention times and operating conditions for ternary systems of the kind presented in this paper and is the basis for extracting isotherms from the data. This appendix provides a summary of the parameter estimation procedure used for this work.

If an explicit function (containing a set of adjustable parameters) of the vapor-phase mole fractions can be used to describe each dry-basis sorption surface, then the procedure is straightforward. For each vapor-phase composition the partial derivatives in eq 2 can be easily calculated from their analytical expressions obtained from the isotherm functions. Then the retention times for the two peaks can be calculated as the two roots of this polynomial equation and compared with the experimental times. This comparison can be made over an entire composition grid in a least-squares sense by calculating an appropriate objective function whose minimization gives an optimum set of adjustable parameters. The objective function used for this work is

$$J = \sum_{\substack{\text{all}\\ \text{compositions}}} \left[\left(\frac{t_{r1,\text{calcd}} - t_{r1,\text{exptl}}}{t_{r1,\text{exptl}}} \right)^2 + \left(\frac{t_{r2,\text{calcd}} - t_{r2,\text{exptl}}}{t_{r2,\text{exptl}}} \right)^2 \right] \quad \text{(A-1)}$$

where dividing each retention time residual by the experimental time weights the residuals approximately in accordance with experimental errors.

The optimization also can be performed if the equations are implicit functions rather than explicit functions of the stationary-phase or gas-phase concentrations, as is the case for the polymer solution theories. These solution theory equations for the activity of a component in polymer solution (Table IV) can be combined with an equation for the vapor phase[23]

$$a_i^s = \frac{f_i^v}{f_i^\circ} = \frac{y_i P \exp[(2/v) \sum_{j=1}^{n} y_j B_{ij}][1/Z_{\text{mix}}]}{P_i^{\text{sat}} \exp[B_{ii} P_i^{\text{sat}}]} \quad \text{(A-2)}$$

to give a relation between an implicit function of vapor-phase composition (mole fractions) and an implicit function of stationary-phase composition (expressed variously as volume fractions, segment fractions, or site fractions, depending on the theory) for each component considered.

Although more complicated than for the explicit functions discussed above, extracting isotherms using these theories is identical in concept. For ternary polymer/solvent 1/solvent 2 systems these theories have three adjustable parameters that represent the three possible binary interactions (one solvent/solvent interaction parameter and two polymer/solvent interaction parameters). Initial guesses for the parameters allow solution of the set of two simultaneous equations (A-2) to obtain the stationary-phase compositions of the two sorbing components (the vapor-phase compositions are known experimentally). Hence, choosing the parameters is equivalent to defining the sorption isotherms from which can be calculated the isotherm partial derivatives and consequently the retention times (eq 2).

The primary complications in this procedure are two. First, the activity equations A-2, one for each sorbing species, are functions implicit in the stationary-phase concentrations that cannot be solved explicitly for these concentrations in terms of the vapor-phase activities. Second, the stationary-phase concentration definition used in these equations is different from that used in developing the chromatographic relations, and conversion from one definition to the other must be made.

In spite of these problems, however, it is possible to obtain explicit relations for the isotherm partial derivatives required for eq 2 in terms of the "natural" partial derivatives of the activity functions for the vapor and stationary phases. For a ternary system where there are two sorbing species, these are given by the matrix equation

$$\beta = \frac{1}{\phi_P^2} \lambda \cdot \mathbf{C} \cdot \mathbf{A}_s^{-1} \cdot A_v \quad \text{(A-3)}$$

The more general multicomponent result is given by Ruff et al.[10] In this equation the various arrays are defined as (for segment fraction stationary-phase concentrations)

$$\beta = \begin{pmatrix} \frac{\partial g_1}{\partial y_1} & \frac{\partial g_1}{\partial y_2} \\ \frac{\partial g_2}{\partial y_1} & \frac{\partial g_2}{\partial y_2} \end{pmatrix}; \quad \beta_{ij} = \frac{\partial g_i}{\partial y_j}$$

$$\lambda = \begin{pmatrix} \lambda_1 & 0 \\ 0 & \lambda_2 \end{pmatrix} = \begin{pmatrix} \frac{v^*_{psp}}{M_1 v^*_{1sp}} & 0 \\ 0 & \frac{v^*_{psp}}{M_2 v^*_{2sp}} \end{pmatrix}$$

$$C = \begin{pmatrix} (1-\Psi_2) & \Psi_1 \\ \Psi_2 & (1-\Psi_1) \end{pmatrix}$$

$$\mathbf{A_s} = \begin{pmatrix} \left(\frac{\partial a_1^s}{\partial \Psi_1} - \frac{\partial a_1^s}{\partial \Psi_p}\right) & \left(\frac{\partial a_1^s}{\partial \Psi_2} - \frac{\partial a_1^s}{\partial \Psi_p}\right) \\ \left(\frac{\partial a_2^s}{\partial \Psi_1} - \frac{\partial a_2^s}{\partial \Psi_p}\right) & \left(\frac{\partial a_2^s}{\partial \Psi_2} - \frac{\partial a_2^s}{\partial \Psi_p}\right) \end{pmatrix}$$

$$\mathbf{A_v} = \begin{pmatrix} \left(\frac{\partial a_1^v}{\partial y_1} - \frac{\partial a_1^v}{\partial y_3}\right) & \left(\frac{\partial a_1^v}{\partial y_2} - \frac{\partial a_1^v}{\partial y_3}\right) \\ \left(\frac{\partial a_2^v}{\partial y_1} - \frac{\partial a_2^v}{\partial y_3}\right) & \left(\frac{\partial a_2^v}{\partial y_2} - \frac{\partial a_2^v}{\partial y_3}\right) \end{pmatrix}$$

The λ_i are the conversion factors from segment fractions to dry-basis concentrations. The polymer molecular weight is not required since conversion is to mass of polymer and not moles.

As an example, if the Flory–Huggins segment fraction model is used, then the various activity function partial derivatives are

$$\left(\frac{\partial a_i^s}{\partial \Psi_j}\right) = \delta_{ij}\Gamma_i + a_i^v\left(1 - \frac{r_i}{v_j} + \chi_{ij} - \sum_k \Psi_k \frac{r_i}{r_j}\chi_{jk}\right)$$

and

$$\left(\frac{\partial a_i^v}{\partial y_j}\right) = \delta_{ij}\gamma_i + 2\frac{a_i^v P}{RT}(B_{ij} - \sum_k y_k B_{kj})$$

Notation

a_i^s	activity of component i predicted by stationary-phase equation of state (solution model)
a_i^v	activity of component i predicted by vapor-phase equation of state
B_{ij}	second virial coefficient
$\mathbf{b}_n^*$	$1 \times (n-1)$ vector of sorption derivatives for component n
f_i^v	fugacity of component i in vapor
f_i°	fugacity of reference state
g	dry-basis sorption isotherm, moles sorbed per mass of dry polymer
$G_{ii}/\bar{V}i$	cluster function
$\mathbf{I}$	identity matrix
M	molecular mass (solution theories)
M_s	total mass of polymer in the column
n	total number of components in stationary phase
N	total molar flow rate
P	absolute pressure
P_i^{sat}	saturation pressure of pure i
$P\beta$	$-(P/V)(\partial V/\partial P)_T$
$\tilde{p}$	reduced pressure, $\tilde{p} = p/p^*$; $\tilde{p}_i$ for component i in a mixture
p^*	characteristic pressure; p_i^* for component i in a mixture
p_{ij}^*	binary interaction parameter for the simplified Flory model
Δp_{ij}^*	binary interaction parameter for the lattice fluid model
R	universal gas constant
r	mixture average segments per molecule
r_i	number of segments per molecule for component i in the mixture (both Flory and Sanchez–Lacombe) or for pure component i (Flory)
r_i°	number of segments per molecule for pure component i (lattice fluid model)
s	number of intermolecular contact sites per segment (Flory theory)
T	absolute temperature
$T\alpha$	$(T/V)(\partial V/\partial T)_P$
$\tilde{T}$	reduced temperature, $\tilde{T} = T/T^*$; $\tilde{T}_i = T/T_i^*$ for component i in a mixture
T^*	characteristic temperature; T_i^* for component i in a mixture
t_r	net retention time of peak
v_{sp}	specific volume
$\tilde{v}$	reduced volume, $\tilde{v} = v/v^*$; $\tilde{v}_i^* = v_i/v_i^* = v_{isp}/v_{isp}^*$ for component i
v^*	characteristic close-packed volume per segment
v_{sp}^*	characteristic close-packed volume per unit mass
w_i	stationary-phase weight fraction of component i
X_{ij}	i–j binary interaction parameter for the Flory model
y_j	mole fraction of component j in vapor phase
$\mathbf{y}_n^*$	$1 \times (n-1)$ vector of vapor-phase mole fractions
$\mathbf{Y}^*$	$(n-1) \times (n-1)$ matrix of vapor-phase mole fractions
Z_m	mixture compressibility

Subscripts and Superscripts

C	cyclohexane
$i, j, \ldots$	species $i, j, \ldots$
IPA	isopropyl alcohol
n-hep	n-heptane
p	denotes polymer
s	stationary phase (see eq 1)
sp	per unit mass
*	denotes steady-state value (chromatography theory) or characteristic property (solution theories)

Greek Letters

β	matrix of sorption derivatives of components 1 through $(n-1)$
β_{ij}	$(\partial g_i/\partial y_j)_{T,P,y_k}$; $k \neq j$
Γ_i	segment fraction activity coefficient $= (a_i/\Psi_i)$
γ_i	mole fraction activity coefficient
δ_{ij}	Kronecker delta ($\delta_{ij} = 0$ for $i \neq j$ and $\delta_{ij} = 1$ for $i = j$)
θ_i	site fraction (Flory model)
$\tilde{\rho}_i$	reduced density, $\tilde{\rho} = 1/\tilde{v}$; $\tilde{\rho}_i = 1/\tilde{v}_i$ for component i
ϕ_i	volume fraction
χ_{ij}	interaction parameter of Flory–Huggins model
Ψ_i	segment fraction
Ω_i	weight fraction activity coefficient of component i

Registry No. APP, 9003-07-0; IPA, 67-63-0; n-heptane, 142-82-5.

References and Notes

(1) Smidsrød, O.; Guillet, J. E. *Macromolecules* **1969**, *2*, 272.
(2) Flory, P. J. *J. Chem. Phys.* **1942**, *10*, 51.
(3) Sanchez, I.; Lacombe, R. H. *J. Phys. Chem.* **1976**, *80*, 1352.
(4) Sanchez, I.; Lacombe, R. H. *Macromolecules* **1978**, *11*, 1145.
(5) Bonner, D. C.; Brockmeier, N. F. *Ind. Eng. Chem. Process Des. Dev.* **1977**, *16*, 180.
(6) Dincer, S.; Bonner, D. C.; Elefritz, R. A. *Ind. Eng. Chem. Fundam.* **1979**, *18*, 54.

(7) Ching, D. W. W., M.S. Thesis, Texas A&M University, College Station, TX, 1978.
(8) Ruff, W. A.; Glover, C. J.; Watson, A. T.; Lau, W. R.; Holste, J. C. *AIChE J.*, in press.
(9) Glover, C. J.; Lau, W. R. *AIChE J.* **1983**, *29*, 73.
(10) Ruff, W. A.; Glover, C. J.; Watson, A. T. *AIChE J.*, in press.
(11) Deans, H. A.; Horn, F. J.; Klauser, G. *AIChE J.* **1970**, *16*, 426.
(12) Lau, W. R.; Glover, C. J.; Holste, J. C. *J. Appl. Polym. Sci.* **1982**, *27*, 3067.
(13) Huggins, M. L. *Ann. N. Y. Acad. Sci.* **1942**, *43*, 1.
(14) Flory, P. J. *J. Am. Chem. Soc.* **1965**, *87*, 1833.
(15) Bonner, D. C.; Prausnitz, J. M. *AIChE J.* **1973**, *19*, 943.
(16) Zimm, B. H. *J. Chem. Phys.* **1953**, *21*, 934.
(17) Phong-Nguyen, H.; Delmas, G. *Macromolecules* **1979**, *12*, 740.
(18) Ochiai, H.; Ohashi, T.; Tadokoro, Y.; Murakami, I. *Polym. J. (Tokyo)* **1982**, *14*, 457.
(19) Brockmeier, N. F.; McCoy, R. W.; Meyer, J. A. *Macromolecules* **1972**, *5*, 464.
(20) Bondi, A. A. *J. Phys. Chem.* **1964**, *68*, 441.
(21) Lau, W. R., M.S. Thesis, Texas A&M University, College Station, TX, 1980.
(22) Sanchez, I.; Lacombe, R. H. *J. Polym. Sci., Polym. Lett. Ed.* **1977**, *15*, 71.
(23) Prausnitz, J. M. *Molecular Thermodynamics of Fluid Phase Equilibria*, 1st ed.; Prentice-Hall: Englewood Cliffs, NJ, 1969; Chapter 7.

Regions of Fickian Diffusion in Polymer–Solvent Systems

J. S. Vrentas,* J. L. Duda, and W. J. Huang

Department of Chemical Engineering, The Pennsylvania State University, University Park, Pennsylvania 16802. *Received January 29, 1986*

ABSTRACT: Oscillatory and step-change sorption experiments are used to help locate regions of Fickian diffusion for amorphous polymer–solvent systems. Sorption experiments are characterized by using a dimensionless group, the diffusion Deborah number, and sorption data are reported for water and methanol diffusion in poly(vinyl acetate). It is found that there are at least two Fickian regions for polymer–solvent diffusion which can be observed by varying the time scale of the experiment at fixed temperature, concentration, and polymer molecular weight. A low-frequency region is a viscous Fickian diffusion region, and a high-frequency region is a rubberlike elastic Fickian diffusion region.

It is well-known that diffusion processes in polymer–solvent systems often do not follow the laws of the classical theory of molecular diffusion.[1,2] There is thus not only considerable interest in understanding the anomalous effects observed in mass-transfer processes for polymer–penetrant systems but also interest in anticipating conditions for which it is possible to utilize the classical or Fickian theory in analyzing the diffusion process. In general, Fickian diffusion can be observed for polymer–solvent systems at sufficiently high temperatures and solvent concentrations since the polymer–solvent system behaves like a purely viscous fluid mixture under such conditions. In addition, it is commonly accepted[3-7] that diffusion at low penetrant concentrations below the polymer glass transition temperature can be analyzed by using the classical theory since the system appears to have the properties of an elastic solid. At intermediate temperatures and concentrations, a polymer–solvent mixture can exhibit anomalous or non-Fickian diffusion phenomena which are caused by viscoelastic effects in the polymer–penetrant system. As a penetrant diffuses through a polymeric material, the polymer chains must take on new conformations consistent with the new penetrant concentration. If this polymer chain rearrangement occurs on a time scale comparable to that of the diffusion process, behavior which is not consistent with classical diffusion theory will result. It is thus possible to observe widely different diffusional behavior in polymer–solvent systems by performing experiments that traverse large enough ranges of temperature, concentration, and polymer molecular weight.

Another way of investigating the diverse behavior exhibited in diffusion processes for polymer–solvent systems is to conduct a series of experiments by varying the characteristic time of an experiment at fixed temperature, concentration, and polymer molecular weight. This can be done for step-change sorption experiments by changing the thickness of the sample[8] and for oscillatory sorption experiments by varying the oscillation frequency.[9] Similarly, different characteristic experimental times can be obtained in quasi-elastic light-scattering experiments by varying the momentum-transfer range.[10,11] The principal objective of this study is to use oscillatory diffusion experiments, carried out at different oscillation frequencies and at fixed temperature, average concentration, and polymer molecular weight, to help locate regions of Fickian diffusion for amorphous polymer–solvent systems. The utilization of a dimensionless group, the diffusion Deborah number, in the characterization of sorption experiments is discussed in the second section of the paper, and a description of oscillatory and step-change sorption experiments is presented in the third section of the paper. Data for the water–poly(vinyl acetate) (PVAc) and methanol–PVAc systems are presented and discussed in the fourth section of the paper.

Diffusion Deborah Number

The presence of Fickian diffusion in polymer–solvent systems can be anticipated by comparing the rate of diffusion to the rate of rearrangement of polymer molecules. In the absence of externally induced flow in a concentration field, all deformations are the direct result of concentration gradients. In such cases, the nature of the diffusional transport in a polymer–solvent system can conveniently be ascertained by defining a diffusion Deborah number $(DEB)_D$ as the ratio of a characteristic time λ_m of the fluid to the characteristic time θ_D of the diffusion process:[12-14]

$$(DEB)_D = \lambda_m/\theta_D \tag{1}$$

This dimensionless group will provide a useful characterization of a diffusion process if single values of θ_D and λ_m suffice to give an adequate representation of a particular mass-transfer operation. This point will be discussed further below.

For very small values of the diffusion Deborah number, molecular relaxation is much faster than the diffusive transport, and the diffusion process involves what is es-

0024-9297/86/2219-1718$01.50/0